

Atrioventricular blood flow simulation based on patient-specific data

Viorel Mihalef¹, Dimitris Metaxas¹, Mark Sussman², Vassilios Hurmisiadis³,
and Leon Axel⁴

¹ CBIM Center, Rutgers University, NJ, USA

² Department of Mathematics, Florida State University, FL, USA

³ Primal Pictures Ltd, London UK

⁴ Department of Radiology, New York University, NY, USA

Abstract. We propose a new framework for simulating blood flow inside the heart, usable with geometric models of the heart from patient-specific data. The method is geared toward realistic simulation of blood flow, taking into account not only heart wall motion but also valve motion. The simulator uses finite differences to discretize a domain that includes a functional model of the left ventricle and the left atrium of the heart. Navier-Stokes equations are robustly solved throughout the simulation domain, such that one-way momentum transfer between the heart model and the blood is enforced. The valve motion was timed to correspond to valve motions obtained from MRI. The final simulation results are qualitatively consistent to those from MR phase contrast velocity mapping, including high-velocity flow to the aorta during systole and toroidal vortex formation past the mitral valve during diastole.

1 Introduction

As a result of a continuous increase in computational and imaging resources, blood flow simulation inside the heart is becoming a more and more precise scientific endeavor, greatly enhancing its possible use as a clinical application. This paper presents a framework for blood flow simulation in the heart that is flexible but simple enough to be part of a future clinical application suite. The method has been already introduced to computer graphics by [7] and here we present some enhancements and its application to heart blood flow simulation.

One of the first papers to tackle patient-specific simulation of left ventricular blood flow was [2]. The heart model used was only including the left ventricle and was imposing boundary conditions in the valve regions. Our method takes as input a sequence of full 3D heart meshes (including valves, atria and ventricles), then generates, as an intermediary step, a velocity field to be used as a boundary condition for the simulation, and then runs our proprietary Navier-Stokes solver to generate the blood flow dynamics. Such an approach is usually characterized as one-way momentum transfer. We are also working on a two-way momentum transfer approach, that will take into account the response of the flow on the heart walls, to be presented in the near future.

For obtaining realistic simulations our method relies on the use of a fairly complete heart model (in this case the left side), based on the one proposed by [1], that is immersed in a 3D computational box and allowed to transfer its momentum to the fluid inside and/or outside the heart model (our focus in this paper is the inside). Some advantages of this approach are relative computational simplicity while allowing geometric and topologic complexity, and also the possibility of using predefined models obtained from high quality MR data, or artificial heart models.

One of the main appeals of our method is that it allows for more complex/realistic setups than previous frameworks like [5, 6, 9], while also offering a comprehensive simulation platform that could take into account heart wall deformation as well. This is due to our use of the Standard Coupler Interface (SCI) framework which decouples fluid and (possibly deformable) solid simulation/implementation and our use of a “cartesian grid” (embedded boundary) method for treating the embedded heart. With such an approach one has less to worry about how to design boundary conditions or prescribe inflow/outflow velocity or pressure profiles for variable moving surfaces as in [5] or [9], and can (and should) focus on the geometric model of the heart, with the possibility of considering in more depth its mechanical deformation properties. Our method proved to be robust, regardless of the specified motion of the heart walls and valves.

In our work, the valves open and close progressively rather than instantaneously. This, combined with the presence of the mitral valve, led in our simulations to the formation of an annular vortex ring during early diastole. We note that [9] did not observe such a vortex formation, using only a circular ventricular inflow opening.

In this work we use a geometrically more realistic (MRI based) model than the simple one used by [6]. However, we should underline that an even more realistic simulation would have to use a twisting ventricle model obtained from tagged MRI, as reported by [10], with appropriately well resolved ventricular walls that can ensure the delivery of the wall rotational momentum to the blood. Finally, our model could be enhanced by the consideration of the mechanical deformation properties of the cardiac walls and of the valves.

In the following we present our simulation framework in section 2, along with the results obtained using it in section 3.

2 Simulation method

Our simulation framework embeds the heart model in a rectangular box domain and solves the Navier-Stokes with a variable density throughout the domain, by prescribing the velocity in the solid/fluid cells as a boundary condition affecting directly the pressure Poisson solver. The domain outside the heart may be thought of as a passive body circulatory system. In this work the heart motion is completely predefined, and, as a consequence, fluid flow does not influence its motion. Our solver setup uses the so called Standard Coupler Interface (SCI)

framework which decouples Fluid and Solid simulation and implementation. In this paper the Solid code has quite simple tasks to handle, namely to pass at the appropriate time step the position and velocity of the heart and vessel stubs walls to the Fluid code, which uses this info to enforce the appropriate boundary conditions. This transfers in effect the heart kinematics to the blood flow. In a future model, which the SCI framework can handle naturally, we will also transfer momentum back from the fluid to the heart walls. The SCI framework works thus as follows: at any computational step

- the Fluid code advances flow calculation
- the Solid code advances body and passes velocity and position information to the Fluid code

In the rest of this section we present the fluid computation and the solid representation in more detail.

2.1 Fluid flow simulation

The governing equations consist of the Navier-Stokes equation, and continuity condition:

$$\rho \frac{D\mathbf{u}}{Dt} = -\nabla p + \mu \Delta \mathbf{u}$$

$$\nabla \cdot \mathbf{u} = 0$$

The physical parameters are here the blood density $\rho_{liquid} = 1050 kg/m^3$ and the dynamic viscosity $\mu = 4 mPa \cdot s$. \mathbf{u} is the velocity, p the internal pressure, and $\frac{D}{Dt}$ is the material (advective) derivative,

$$\frac{D}{Dt} \equiv \frac{\partial}{\partial t} + \mathbf{u} \cdot \nabla$$

At the beginning of each time step, we are given the velocity of the liquid \mathbf{u} and the velocity of the solid \mathbf{u}^{solid} . We define a solid/fluid level set function ψ that will be used to distinguish between the solid and the liquid phase. The face centered density is defined (given here in 2D, for simplicity, but the 3D extension is trivial) as

$$\rho = \begin{cases} \rho_{liquid} & \text{if } \psi_{i+1/2,j} > 0 \\ 10^{15} & \text{otherwise} \end{cases}$$

For each time step, one does the following:

1. calculate provisional advective states for cell centered variables,

$$\frac{D\mathbf{u}}{Dt} = 0 \quad \frac{D\psi}{Dt} = 0$$

2. pressure correction step, in which we take into account the solid velocity.

$$\mathbf{u}_{i+1/2,j}^* = \begin{cases} \mathbf{u}^{\text{solid}}_{i+1/2,j} & \text{if } \psi_{i+1/2,j} \leq 0 \\ \mathbf{u}_{i+1/2,j} & \text{otherwise} \end{cases} \quad (1)$$

A pressure is derived which minimizes the quantity:

$$|dt\nabla \cdot \frac{\nabla p}{\rho} - \nabla \cdot \mathbf{u}^*|. \quad (2)$$

3. update the density using the current values of the level set, then update the liquid velocity

$$\mathbf{u}_{i+1/2,j} = \begin{cases} \mathbf{u}^{\text{solid}}_{i+1/2,j} & \text{if } \psi_{i+1/2,j} \leq 0 \\ \mathbf{u}_{i+1/2,j} - \frac{\nabla p}{\rho} & \text{otherwise} \end{cases} \quad (3)$$

2.2 Solid wall treatment

Each solid mesh corresponds to a specific time step in a 1Hz cardiac cycle. The left side of the heart chambers and vessel stubs geometry has been obtained from high resolution MRI imaging, as reported by [1]. A volume variation graph for both the left atrium and the left ventricle shows behaviour consistent with the classical physiological curves, and is presented in figure 2. In the same work, approximate fiber orientations from the University of Auckland canine fiber dataset were used to approximate the tangential motion of the ventricular wall. Corresponding valve geometry was modeled as well, and for this paper it has been modified and synchronized to better correspond to the cardiac cycle, as summarized in figure 1.

We used the doubly-wetted specification (as defined by [7]) for the description of the solid. This means, in short, that the original solid mesh is replaced inside the solver by another mesh defined as the dx level of the distance function of the mesh. In effect, this displaces the mesh dx away from the original one in both directions along the normals, and the smaller the grid size dx becomes, the better the approximation of the original geometry is. A geometric advantage of such a setup is that one can afford overlapping or holes of size less than dx inside the original mesh. A limitation is that one drops to first order accuracy when it comes to approximating the original mesh, and any sharp or small features (like ventricular wall creases) may be smoothed out for large grid steps.

2.3 Numerical considerations

We used free-slip conditions along the computational box boundary. The heart walls impose automatically a no-slip condition on the fluid by means of equations (1) and (3). When both valves are closed our geometry does exhibit some volume variation, however our solver is robust. In order to accomplish this, we relax the incompressibility condition so that we fulfill $\nabla \cdot \mathbf{u} = A$, where A is a small nonzero constant. From the divergence theorem we have for example that $A =$

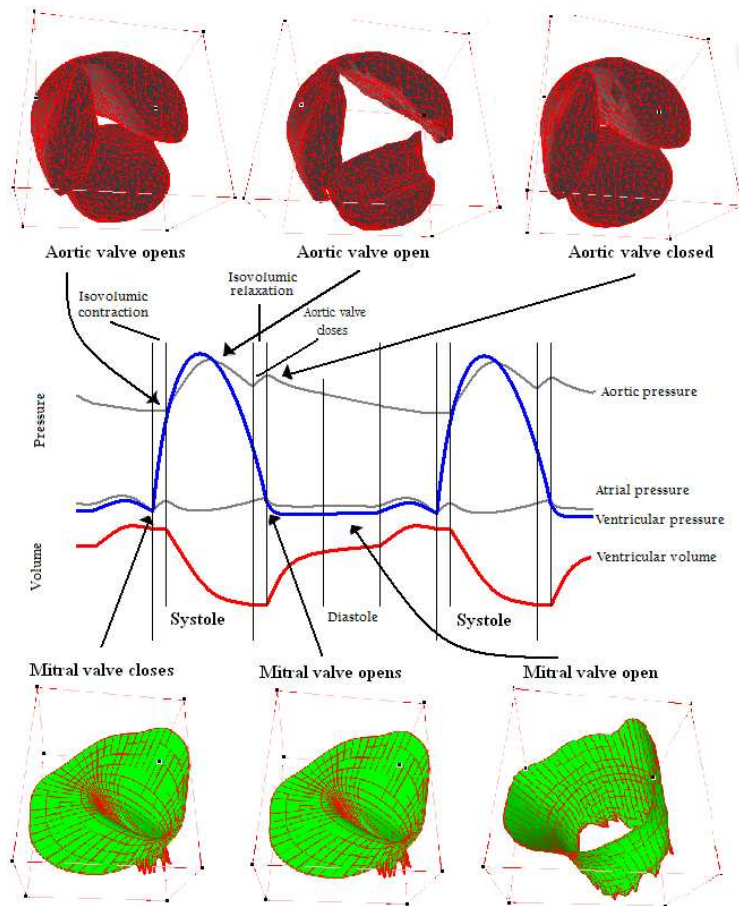


Fig. 1. A general heart cycle and specific keyframes of our aortic and mitral valves.

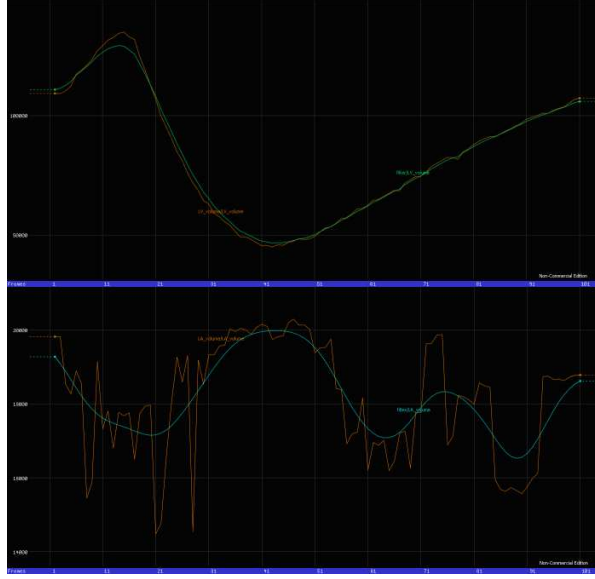


Fig. 2. Volume variation over one cardiac cycle of the left ventricle and atrium.

$\frac{1}{vol(D)} \int_{\partial D} \mathbf{u} \cdot \mathbf{n}$, where $vol(D)$ is in our case the volume of the closed ventricular domain. We therefore solve a modified Poisson equation, namely $dt \nabla \cdot (\frac{1}{\rho} \nabla p) = \nabla \cdot \mathbf{u}^* - A$.

The projection method that we use for solving the Navier-Stokes equations does not include tracking the pressure in time. This, together with the possible gauge shift in the pressure values induced by the topological changes of the heart wall, complicates the issue of computing temporally coherent pressure values. We did notice however that during the various topologically stable stages, the pressure did behave as expected. For example, the pressure rose during the isovolumic contraction, and went down during the isovolumic relaxation. Similarly, the pressure remained fairly constant during diastole and rose and then dipped during systole.

3 Results

To perform our heart simulation we set up a model of the inner side of the left ventricle connected with the aorta and with the left atrium and its associated vessel stubs. Both aortic and mitral valves were in place, timed to open and close as visible in Figure 1. In particular, they were both closed during the isovolumic phases, and were smoothly interpolated from the closed positions to their full open extent (as noted, this is in contrast with previous work like [5,

[9], but similar to [6]). Our code spent an average of 6 hours to compute each cardiac cycle, computing 200 time steps in about 1.8 minutes per time step, on a 2.4GHz Quad Core PC. The grid size was $96 \times 96 \times 96$ for the results presented here. We have also run a $64 \times 64 \times 64$ simulation with qualitatively similar results, although it also showed the possible limitations of the doubly-wetted approach. Namely, when using the coarser mesh, the strong grid dependence of the small holes, including the vessel stubs, led to partial occlusion of the smaller vessels, and to diameter reduction of the aorta, so that the ventricular pressure increased greatly during systole, and led to too large aortic velocities. This is a numerical rather than a methodological artifact, and can be completely avoided once the grid spacing is chosen small enough. In our specific case for example, 96^3 was a fine enough grid, as proved by numerically consistent results obtained subsequently on a 128^3 grid.

Figure 3 shows several representative images from the main simulation. The images tell a story consistent with the MR velocity analysis from classic papers like [4], or [3] (who used phase contrast MRI). One sees several vortex formations during early diastole, with a main annular vortex shooting toward the apex, and subsiding in strength right before the atrial systole. The formation mechanism of the main vortex seems to be determined by the blood shear induced by the valve itself, as indicated by [4]. In figure 4 we show the vortex position at an early diastolic time step. Next, the atrial systole increases again the ventricular inflow velocities and contributes to short-lived new vortex formation. After an instant of isovolumic calm, the pressure buildup forces strong ejection of blood through the aorta, once the aortic valve opens. In the beginning of the systolic phase, the velocities (especially the ones inside the aorta) are the largest across the whole cycle. Towards the end of the systole, the ventricular velocities subside in magnitude, while the ones in the aorta remain quite high. During the subsequent isovolumic relaxation, the velocities decrease greatly, only to increase again with the start of a new cycle.

In terms of validation, the use of magnetic resonance imaging (MRI) methods for 3D mapping of velocities within the heart, at multiple phases of the cardiac cycle, is already possible with conventional MRI systems and their associated software (or with relatively minor modifications). Although the time required for acquiring the large amount of associated imaging data is currently too long for routine incorporation within clinical cardiac MRI examinations, it is already feasible for research purposes. Thus, we will be able to obtain suitable in-vivo 7D velocity data in the same subjects from whom the 4D cardiac structural data is acquired for use in the CFD calculations, for comparison with and validation of the theoretical velocity fields computed from the MRI-derived boundary conditions. With the ongoing and expected continual advances in the speed of cardiac MRI, it is likely that this method of blood flow mapping will become faster and more accurate, and that it will find increasing clinical application. Thus, the insights into the physics of the blood flow patterns that can potentially be provided by these CFD results will be expected to be useful both for advancing our

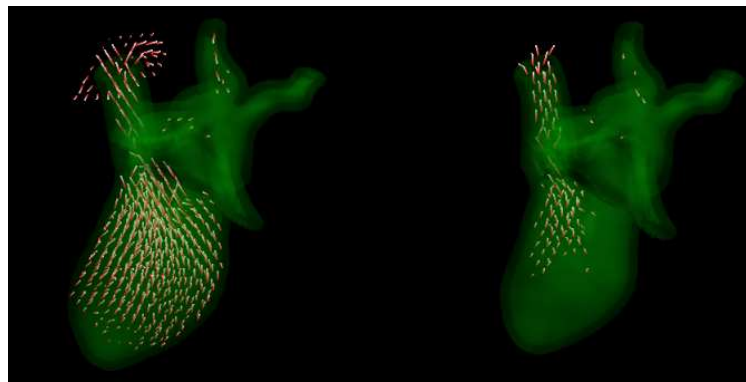
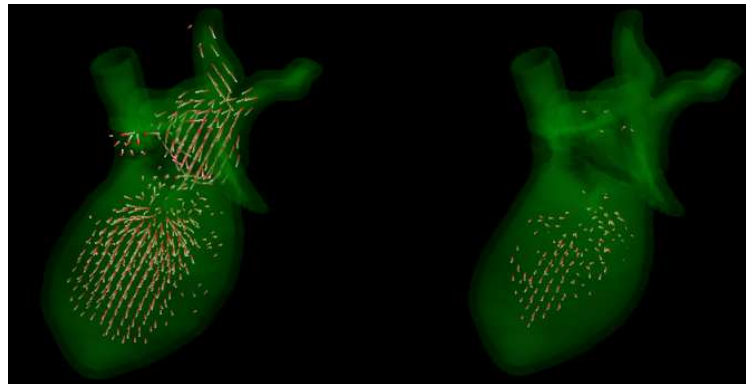
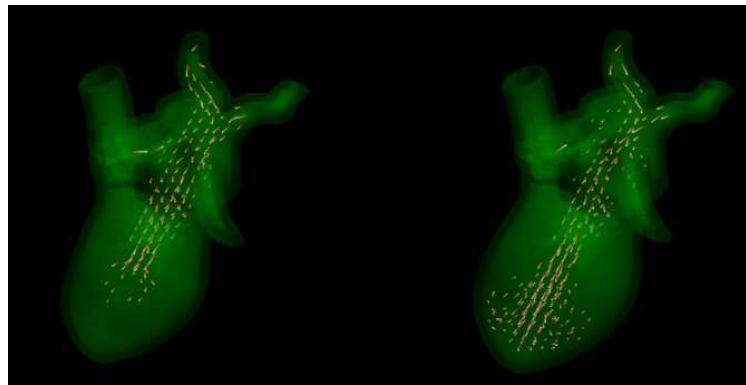


Fig. 3. Our heart cycle simulation in different stages. From left to right, top row: early diastole, diastole with annular vortex formation. Middle row: atrial systole, isovolumic contraction. Bottom row: early systole, late systole.

understanding of normal and abnormal physiologic process and for improving the care of individual patients.

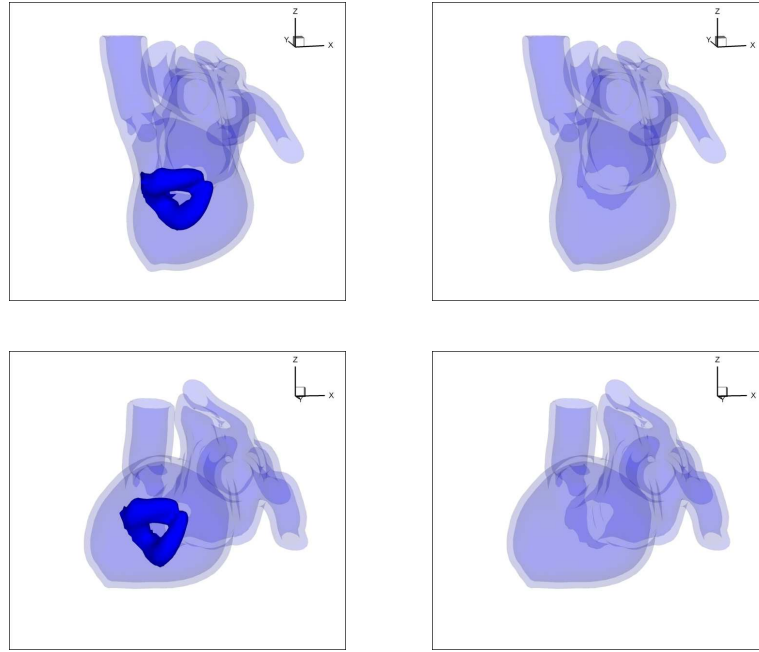


Fig. 4. Ring vortex formation at a given step early diastolic stage ($t=0.625\text{sec}$, in a 1 second cycle). From left to right, and top to bottom: view 1, with ring, view 1 without ring, view 2, with ring, view 2 without ring. The ring is visualized as a fixed vorticity isosurface right below the mitral valve, with all other vorticity isosurfaces (present mainly on the mitral valve and the atrial vessels) removed for clarity.

4 Conclusion

We have presented a novel computational approach for simulating blood flow inside the heart that is simple yet versatile. We have used it to perform a medium size numerical simulation using a relatively complete model of the left side of the heart, including animated models of the aortic and mitral valves, and aortic and left atrial vessel stubs. We found the main characteristics of the resulting simulation to be consistent with the ones published in the literature, from general flow direction and relative size, to specific vortex formation. We are working on extending our framework with a two-way momentum transfer mechanism, and on updating the heart model with smaller intraventricular structures from MRI data, as well as more realistic twisting motion based on tagged MRI.

Acknowledgments. The authors want to thank the reviewers for their very useful suggestions and questions that led to substantial improvement of the original exposition. The first author thanks Iuliana Radu for her help in generating Figure 1. The first two authors were supported by NSF grant 0702591.

References

1. Hurmisiadis, V., Briscoe, C. - A functional heart model for medical education, Proceedings of FIMH 2005.
2. Jones, T., Metaxas D. - Patient-Specific Analysis of Left Ventricular Blood Flow, Proceedings of MICCAI 1998, 156–166
3. Jung B, Schneider B, Markl M, Saurbier B, Geibel A, Hennig J. - Measurement of left ventricular velocities: phase contrast MRI velocity mapping versus tissue-doppler-ultrasound in healthy volunteers. *J Cardiovasc Magn Reson.* 2004;6(4):777–783.
4. Kim, Y. H., Walker, P. G., Pedersen, E. M., Poulsen, J. K., Oyre, S., Houlind, K., and Youganathan, A. P. - Left ventricular blood flow patterns in normal subjects: a quantitative analysis by 3-D magnetic resonance velocity mapping, *J. Am. Coll. Cardiol.*, 1995, 26, 224-238.
5. Q. Long, R. Merrifield, and G. Z. Yang, P. J. Kilner and D. N. Firmin, X. Y. Xu - The Influence of Inflow Boundary Conditions on Intra Left Ventricle Flow Predictions, *Journal of Biomechanical Engineering*, 2003, 125, 922–927
6. McQueen D., Peskin C. - A three-dimensional computer model of the human heart for studying cardiac fluid dynamics, *Computer Graphics*, 2000, 34(1)
7. Mihalef, V., Kadioglu, S., Sussman, M., Metaxas, D., Hurmisiadis, V. - Interaction of Multiphase Flow with Animated Models, *Graphical Models*, 2008, 70, 33-42.
8. Peskin, C. S., McQueen, D. M. - Cardiac fluid-dynamics, *Crit. Rev. Biomed. Eng.*, 1992, 20, 451-459.
9. Saber N., Wood N., Gosman A. D., Merrifield R., Yang G.-Z., Charrier C., Gatehouse P., Firmin D. - Progress Towards Patient-Specific Computational Flow Modeling of the Left Heart via Combination of Magnetic Resonance Imaging with Computational Fluid Dynamics, *Annals of Biomedical Engineering*, 2003, 31(1), 42-52.
10. Qian, Z., Metaxas, D., Axel, L. - Learning Methods in Segmentation of Cardiac Tagged MRI, 2007, Proceedings of ISBI